

Cohort aggregation modelling for complex forest stands: Spruce-aspen mixtures in British Columbia

Oscar García

Dasometrics, Concón, Chile

Abstract

Mixed-species growth models are needed as a synthesis of ecological knowledge and for guiding forest management. Individual-tree models have been commonly used, but the difficulties of reliably scaling from the individual to the stand level are often underestimated. Emergent properties and statistical issues limit their effectiveness. A more holistic modelling of aggregates at the whole stand level is a potentially attractive alternative. This work explores methodology for developing biologically consistent dynamic mixture models where the state is described by aggregate stand-level variables for species or age/size cohorts. The methods are demonstrated and tested with a two-cohort model for spruce-aspen mixtures named SAM. The models combine single-species submodels and submodels for resource partitioning among the cohorts. The partitioning allows for differences in competitive strength among species and size classes, and for complementarity effects. Height growth reduction in suppressed cohorts is also modelled. SAM fits well the available data, and exhibits behaviors consistent with current ecological knowledge. The general framework can be applied to any number of cohorts, and should be useful as a basis for modelling other mixed-species or uneven-aged stands.

Keywords: mixed species stands, competition, resource capture, complementarity, forest growth and yield, replacement series

1. Introduction

There is increasing interest in managing existing forest stands with complex structure, comprised of several species and/or age classes, as well as in establishing man-made forests with those characteristics (Groot et al., 2004; Lilles and Coates, 2014; Pretzsch et al., 2015; Kabzems et al., 2016; del Río et al., 2016). Much progress has been made in the design and analysis of experiments or observational studies to predict and understand the development of these heterogeneous stands, but results are often inconclusive and difficult to interpret (Forrester and Pretzsch, 2015). Appropriate mathematical models are needed to synthesize available knowledge and to reliably describe stand dynamics under various growing conditions and silvicultural alternatives.

Email address: garcia@dasometrics.net (Oscar García)

¹©2016. This manuscript version is made available under the CC-BY-NC-ND 4.0 license:
<http://creativecommons.org/licenses/by-nc-nd/4.0/>.

To appear in Ecological Modelling, accepted 24 Oct 2016

DOI: 10.1016/j.ecolmodel.2016.10.020

The conceptually simplest modelling approach for complex stands is at the individual-tree level, representing tree growth and neighborhood interactions that are then aggregated to predict consequences at the stand level. Such individual-based models have a long history in forestry (Reventlow, 1879; Staebler, 1951; Newnham and Smith, 1964), and more recently have become widely used in plant ecology and other fields (Grimm and Railsback, 2005). Individual-tree modelling is by far the prevalent paradigm for complex stands, both for management and for research (Weiskittel et al., 2011b; Pretzsch, 2009). It appears, however, that forest stands can act like *complex systems*, “made up of a large number of parts that interact in a nonsimple way” (Simon, 1962; Sayama, 2015). These systems have (*emergent*) properties at a macroscopic scale (e. g., at the stand level) that are hard to explain simply from microscopic properties (e. g., tree level). Several examples of such difficulties in individual-tree modelling have been identified (Lee and García, 2016): (a) Current models ignore positive spatial tree size correlations induced by heterogeneity in soil nutrients and moisture content, which frequently override the negative correlations expected from neighborhood competition. Either way, the analogy of tree size distributions to probability distributions based on statistical independence is questionable; size distributions are either ill-defined or plot-size dependent, and spatial correlation can introduce serious biases in predicted stand-level quantities (Mitchell-Olds, 1987; Sambakhe et al., 2014). (b) Plasticity allows trees to dynamically adapt their foliage and root distribution according to space availability, causing models based on rigidly fixed tree shapes, locations and allometries to be unrealistic (Strigul et al., 2008). (c) Past competitive interactions are integrated in current tree size (Perry, 1985), and having essentially the same size variable on both sides of tree growth equations is a source of statistical confounding that inflates fit statistics, and causes predictions to be unreliable outside the growing conditions represented in the data. (e) Growth and mortality may be unpredictable at the individual level due to sensitivity to initial conditions that are not precisely known (chaos; García, 2010). It follows that a forest stand is more than a sum of individual trees, and simple bottom-up modelling of tree behavior may fail to adequately reproduce behavior at the stand scale. This can be especially troublesome when growing conditions change over time through disturbances or a varying environment (e. g., Russell et al., 2015).

Complex or chaotic systems can become more predictable if described on a coarser scale through aggregation (Salas et al., 2005; García, 2010). Therefore, whole-stand modelling, with stand-level means or totals as state variables, could be an attractive alternative to individual-tree approaches in forest management. Aggregate values like mean heights, basal area and trees per hectare can be reliably measured and are often adequate for decision-making. If necessary, size distributions may be approximated by top-down disaggregation. Despite the practical limitations of individual-based methods in their current form, they still are valuable research tools that can shed light into the issues mentioned in the previous paragraph.

Whole-stand modelling is well developed for even-aged monocultures (Weiskittel et al., 2011a, Section 4.2), but it has rarely been used for managing complex stands. A notable exception is the work of Moser and associates, who produced growth and yield models projecting aggregates by species or age/size class cohorts (Moser and Hall, 1969; Lynch and Moser, 1986; Atta-Boateng and Moser, 2000). Moser’s models are empirical, entirely data-driven. More mechanistic biologically consistent approaches are desirable for reduced data requirements and for plausible extrapolation. This work aims to explore cohort aggregation methodology through the development of a growth and yield model for spruce-aspen mixed stands named SAM (for Spruce-Aspen Mixtures). The new model takes advantage of existing single-species models for spruce (Scube; García, 2011) and aspen (TAG; García, 2013), extending them to represent the dynamics of two interacting cohorts differing in species and density, and possibly in size and age.

The principles can be generalized to any number of cohorts. SAM is viewed as experimental, given the current gaps in knowledge and information about the dynamics of these forests. Research is still needed to fill those gaps, and possibly improve equations and statistical methods.

Following from the single-species formulations, SAM describes the state of the two-cohort mixture by each cohort's mean height, number of trees per hectare, basal area, and a measure of canopy closure. Modelling is guided by the traditional concept of *growing space* as determining *resource capture* (Monteith, 1994), an abstraction that drives tree growth and mortality. The single-species models are re-written in terms of tree-level means, and stand density is expressed through its reciprocal, the mean growing space per tree. Growing space partitioning in the mixture depends on stand density and species composition, following on the classical work of de Wit (1960). In this instance, de Wit's results were extended to take into account differences in tree height. In addition, I allowed for possible complementarity effects that can increase or decrease resource availability in mixtures compared to monocultures (Larocque et al., 2013; Forrester, 2014). These basic ideas of an equivalence between a mixture and two separate monocultures are illustrated in Fig. 1. Other issues that the modelling must resolve are the relationship between cohort mean heights and the top heights used in the single-species models, and the height growth suppression observed in dominated cohorts.

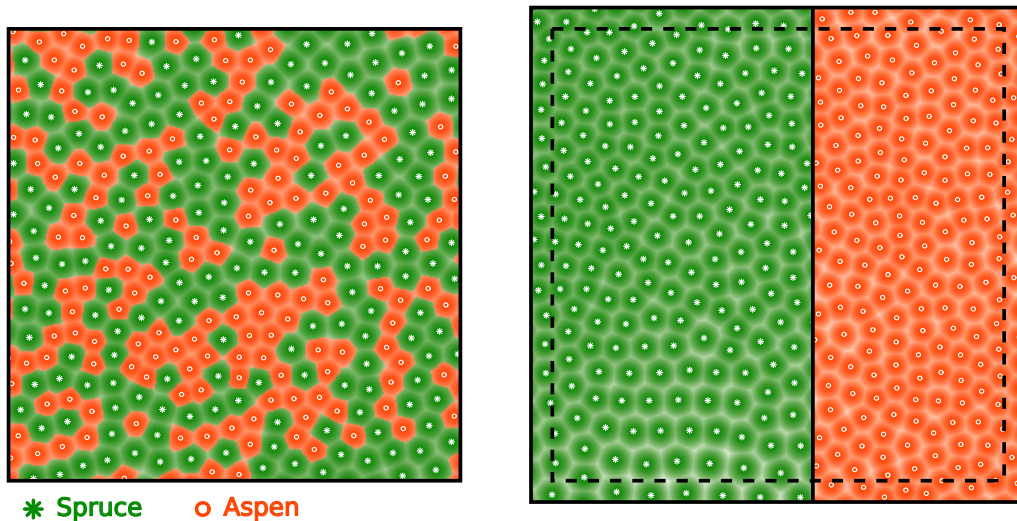


Figure 1: Growing space in a mixture (left), and single-species equivalent (right). The figure assumes equal number of trees and height in both cohorts. Growing space or resource capture per tree is species-dependent. The difference in total area between mixture and monocultures reflects a difference in efficiency due to complementarity effects. Variation with tree size is introduced later in Section 2.3.3. The figure is based on the fitted model parameters.

The next section contains a description of the data and of the single-species models, followed by the growing space partitioning approach. Then top to mean height relationships, height growth suppression, and parameter estimation methods are discussed. *Results* include the parameter values, residuals, and implementation details, as well as examples of model behavior. The article ends with discussion and conclusions. Appendices contain additional details and mathematical derivations.

2. Materials and Methods

2.1. Data

Data was provided by the Forest Analysis and Inventory Branch of the British Columbia Ministry of Forests, Lands and Natural Resource Operations. Initial screening selected all the permanent sample plots from the Province that had re-measurements, and had at least 80% by basal area of either spruce (white spruce, *Picea glauca* [Moench] Voss, or interior spruce, a *Picea glauca* × *engelmannii* hybrid complex) or trembling aspen (*Populus tremuloides* Michx.).

Trees have been measured only above diameter thresholds that vary between 4 and 9 cm. To avoid complications arising from these different measurement standards and the presence of ingrowth, the numbers and diameters of the missing trees were estimated by the procedure described in Section 2.1.3 of García (2013). Only measurements where the estimated basal area of those imputed trees was less than 10% of the total were kept, thus limiting the possible impact of imputation errors. In addition, plots with areas less than 0.04 ha, with less than 600 total trees per hectare, or containing trees from previous generations (*veterans*), were excluded.

Heights usually were only measured on a subsample of trees, and estimated by the Ministry standard height-diameter multi-year regression procedure of Flewelling and de Jong (1994). Tree total stem volume was also computed by standard Ministry methods. Live tree data was summarized by species at the plot level to calculate mean height, trees per hectare, basal area, volume, etc.. Top heights, meaningful for largely single-species stands, were calculated in plots of *A* hectares as the mean height of the 160A – 0.6 largest-diameter trees, interpolating as necessary (García, 1998, 2013).

Growth trends and mortality were examined graphically by species and biogeoclimatic zones (Meidinger and Pojar, 1991). There was substantial representation from the SBS, BWBS, ESSF, ICH, and MS zones. Potential zone effects are interesting because the single-species spruce model Scube was developed with data from the SBS biogeoclimatic zone, while the aspen model TAG used data sources spread over all of western Canada. There were no obvious regional differences in growth patterns within British Columbia, although data variability was high and they cannot be ruled out. Residuals from TAG predictions suggested some under-prediction of basal areas for equivalent heights, and a localization adjustment of that model for British Columbia is described later.

There was no indication in the data of the breakup that is often observed in old-growth aspen stands (Frey et al., 2004; García, 2013). However, similar catastrophic mortality was found in mature spruce, mostly for mean heights above 20–25 m, and apparently unrelated to stand composition (Fig. 2). This spruce breakup does not seem to have been reported in the literature, and merits further research. Its absence in the data from the SBS zone, on which Scube is based, might be explained by a scarcity of tall trees. To avoid dealing with these unpredictable events, measurements with spruce mean height greater than 25 m were omitted. Therefore, the model is not intended to reflect old-growth disintegration or successional processes.

Most measurements have a substantial component of species other than spruce or aspen. Since this is a spruce-aspen model, only measurements with less than 10% of other species by basal area were retained. This threshold was chosen as a compromise between adhering to the two-cohort concept and maintaining an acceptable sample size. Closeness to the two-cohort ideal was enhanced through adjusting plot areas multiplying by the proportion of spruce or aspen, i. e., dividing the previously calculated basal areas and trees per hectare by this quantity. The final simulation software has the option of reversing this adjustment to represent stands with a

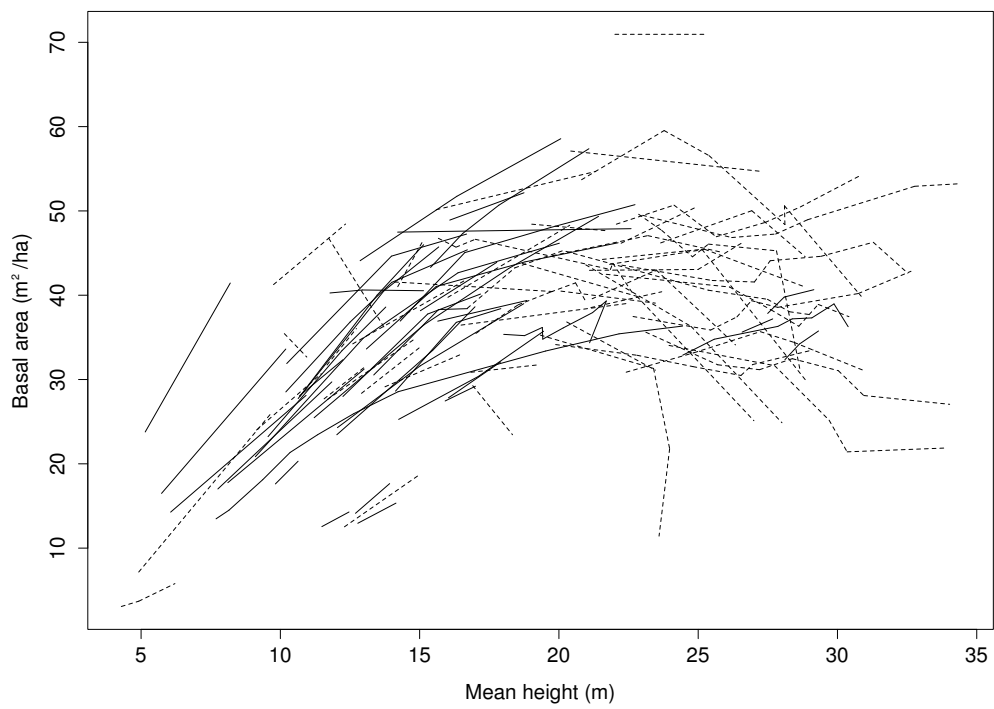


Figure 2: Observed trends of spruce basal area vs height for spruce-dominated plots (> 70% by basal area), indicating heavy mortality in tall stands. Continuous lines are for the SBS and dashed lines are for other biogeoclimatic zones.

moderate proportion of other species. Given the exclusion of multiple species, SAM may be more representative of man-made mixtures than of typical natural stands.

Successive plot measurements were paired for estimating the model parameters. After eliminating some clearly anomalous observations, 118 interval pairs were available, of which 13 had no aspen, 23 had no spruce, and 82 contained both species in various proportions. Tables 1 and 2 give descriptive pair statistics.

Table 1: Growth interval characteristics. 118 measurement pairs from 88 plots.

	Mean	SD	Minimum	Quartile 1	Median	Quartile 3	Maximum
Plot size (ha)	0.0772	0.0232	0.0400	0.0506	0.0809	0.1012	0.1200
Initial year	1986	8.48	1949	1981	1987	1992	1997
Interval length (years)	10.58	2.07	5.00	10.00	10.00	11.00	18.00
Spruce % basal area	45.22	37.48	0.00	8.25	39.51	81.01	100.00
Mean height difference, aspen minus spruce (m)	5.81	4.82	-2.57	2.79	4.85	8.55	20.19

Table 2: Data statistics. 118 measurement pairs from 88 plots.

	Spruce		Aspen		Total	
	Mean	SD	Mean	SD	Mean	SD
Measurement pair means						
Mean height (m)	13.97	4.00	18.70	4.55	16.45	4.90
Trees / ha	785.4	645.9	1039.3	1237.1	1824.8	1067.6
Basal area (m ² /ha)	18.49	16.79	21.26	14.95	39.76	10.22
Arith. mean dbh (cm)	15.76	4.46	18.68	5.74	17.29	5.36
Annual increments						
Mean height (cm/yr)	2.703	0.845	2.345	1.049	2.403	0.785
Trees / ha (trees/ha-yr)	-8.39	14.28	-20.86	28.80	-29.25	29.99
Basal area (m ² /ha-yr)	0.3493	0.3956	0.1850	0.3191	0.5343	0.4144
Arith. mean dbh (mm/yr)	2.779	1.076	2.680	1.251	2.575	0.860

Data for some auxiliary relationships described in the appendices are summarized there.

2.2. Single-species models

Two existing dynamic growth and yield models were used as a starting point, the Scube model for spruce-dominated stands (García, 2011), and the TAG model for aspen-dominated stands (García, 2013). In this section the relevant equations are shown, and are then re-written in a form suitable for application to the mixture cohorts.

Both Scube and TAG have a similar structure, describing a stand through 4 state variables: top height H (m), stand density N (trees/ha), a volume or biomass proxy $W = BH$ (m³/ha) where B is basal area, and a measure of relative site occupancy Ω (dimensionless, not directly

observed). The state evolution is determined by a system of differential equations

$$\frac{dH}{dt} = (p_2/p_3)H[(p_1/H)^{p_3} - 1] \quad (1a)$$

$$\frac{dN}{dH} = -p_4H^{p_5}N^{p_6} \quad (1b)$$

$$\frac{dW}{dH} = p_7\Omega HN^{p_8} + p_9\frac{W}{N}\frac{dN}{dH} \quad (1c)$$

$$\frac{d\Omega}{dH} = p_{10}H(1 - \Omega), \quad (1d)$$

where p_1, \dots, p_{10} are parameters shown in Table 3. The original equations also include a species composition variable, but only the form for pure stands is needed here. Integration produces transition functions that predict state variable values at any future time given their current values.

Table 3: Single-species parameter values

Parameter	Spruce	Aspen ^a
p_1	$283.87q^{0.5137}$	$8.568 + 1342q$
p_2	q	q
p_3	0.5829	1
p_4	4.5759×10^{-15}	0.0004561
p_5	5.009	0
p_6	2.9895	1.6159
p_7	0.5345	0.8560
p_8	0.3	0.2029
p_9	0.3	0.5
p_{10}	2.2×0.023474	0.03
p_{11}	1.815×10^{-6}	1/15605
p_{12}	2.2	2.6

^a The aspen parameters are those in the current version of TAG (<http://forestgrowth.unbc.ca/tag>), with some differing from the published ones.

Eq. (1a) is a self-contained height growth and site index sub-model, in which p_1 and p_2 are functions of a site quality parameter q (Table 3). The value of q may be derived from conventional site index or from biogeoclimatic classification or other methods. In principle, q could vary over time following climate change, but it has been kept constant in the implementations. Mortality, eq. (1b), and wood accumulation, eq. (1c), depend on stand height and density. The occupancy factor Ω reduces growth when the site potential is not fully utilized, e. g., in young open-canopy stands or following thinning. Ω is initialized depending on initial stand density, and tends to 1 according to eq. (1d). Occupancy can be abruptly reduced by thinning.

These models are somewhat atypical in not including basal area or diameter as drivers on the right-hand sides. This is consistent with physiological knowledge, the amount of wood deposited on the stems should not have a significant causal effect on growth or mortality (García, 2011). In addition, the presence of volume or basal area on both sides of a growth equation could cause statistical confounding and extrapolation issues similar to those found in individual-based models (Lee and García, 2016).

In preparation to applying the models to mixture components, we express equations (1b) and (1c) at the level of individual trees, predicting a mean death probability or mortality fraction

$-(dN/dH)/N = -d \ln N/dH$, and the mean $\bar{W} = W/N$. Using $dW/dH = Nd\bar{W}/dH + \bar{W}dN/dH$,

$$\begin{aligned}\frac{d \ln N}{dH} &= -p_4 H^{p_5} N^{p_6-1} \\ \frac{d\bar{W}}{dH} &= p_7 \Omega H N^{p_8-1} + (p_9 - 1) \bar{W} \frac{d \ln N}{dH}\end{aligned}$$

Also, instead of N on the right-hand sides, a biologically more meaningful predictor is the average growing space per tree $\bar{S} = 1/N$, preserving the area units to simplify the presentation (\bar{S} in hectares per tree, although m^2 would be more practical). With these substitutions, equations (1b) and (1c) become

$$\frac{d \ln N}{dH} = -p_4 H^{p_5} \bar{S}^{1-p_6} \quad (2a)$$

$$\frac{d\bar{W}}{dH} = p_7 \Omega H \bar{S}^{1-p_8} + (p_9 - 1) \bar{W} \frac{d \ln N}{dH} . \quad (2b)$$

It is assumed that in this form the models are applicable to the respective species cohort.

Derivatives with respect to t for each cohort can be obtained multiplying equations (2) by dH/dt from eq. (1a). The system of differential equations can then be integrated numerically, given the dependency of the growing space \bar{S} on the other state variables.

For a dominated cohort it was found necessary to multiply eq. (1a) by a height- and density-dependent height growth suppression factor discussed in Section 2.4.2. Therefore, the analytical solution of eq. (1a) from the single-species models cannot be used, and the height growth equation has to be included in the numerical integration.

The occupancy factor Ω can still be calculated from an analytical integral of eq. (1d):

$$\Omega = 1 - (1 - \Omega_0) \exp[-p_{10}(H^2 - H_0^2)/2] . \quad (3)$$

In unmanaged stands Ω can be initialized at breast-height ($H_0 = 1.3$ m) with

$$\Omega_0 = 1 - (1 - \min\{p_{11}/\bar{S}_0, 1\})^{p_{12}} , \quad (4)$$

where \bar{S}_0 may be estimated back-projecting mortality from the first plot measurement (García, 2011, 2013). Most of the development of these stands occurs at near canopy closure ($\Omega \approx 1$), so that the impact of these occupancy equations is usually small.

As mentioned before, TAG had to be localized to better fit the data from British Columbia. This was done by multiplying the right-hand sides of (2) by a localization parameter λ , thus adjusting the mortality rate and the volume or biomass growth relative to height growth.

Some computational aspects are described later in the text. Full details with computer code are contained in the Supplementary Material.

The mixture growing-space relationships are discussed in the next section. Top height is a convenient variable in single-species stands, but its definition and measurement is problematic in mixtures. Therefore, top height is approximated by a function of mean height and growing space (Section 2.4.1). The growth model specification is completed by the height suppression relationships in Section 2.4.2.

2.3. Growing space

Stand density and composition affects competition intensity, with individual growth and mortality depending on the space available to each plant (eq. (2)). In an even-aged monoculture the

mean growing space per plant is simply $\bar{S} = 1/N$. The situation is more complex for species or age/size cohorts, and finding “the most appropriate ways to estimate the species proportions by area in mixed stands” (Dirnberger and Sterba, 2014) has recently received considerable attention in the literature (e. g., Sterba et al., 2014; Pretzsch et al., 2015; del Río et al., 2016). We look for a simple approach appropriate to dynamic modelling and consistent with biological principles.

The next section gives a compact derivation of the relevant results from de Wit (1960). These are extended in Sect. 2.3.2 to represent possible complementarity effects. Section 2.3.3 generalizes the model further to deal with the consequences of different tree sizes.

2.3.1. Interspecific partitioning

The simplest way of apportioning area would be uniformly, ignoring any species or size differences. With the subscripts s and a denoting spruce and aspen, respectively,

$$\bar{S}_s = \bar{S}_a = \frac{1}{N_s + N_a} . \quad (5)$$

Then, the mean individual-tree growth and mortality rate for the spruce component would equal those of a monoculture with a density of $N_s + N_a$ trees/ha, and analogously for aspen. The fraction of the total space captured by spruce, $S_s = N_s \bar{S}_s$, equals its proportion in the mixture, $P_s = N_s / (N_s + N_a)$. A similar approach is used in the extension of TIPSy to mixed-species stands (Ministry of Forests, Lands and Natural Resource Operations, 2013).

More generally, one may expect that the species differ in competitive strength, with one of them intruding into the space of neighbors belonging to the other species. Instead of $\bar{S}_s = \bar{S}_a$, assume that

$$\bar{S}_s = k \bar{S}_a , \quad (6)$$

where k is a *relative crowding coefficient* of spruce with respect to aspen (de Wit, 1960, p. 15). Solving this equation together with the total growing space constraint

$$S_s + S_a = N_s \bar{S}_s + N_a \bar{S}_a = 1 , \quad (7)$$

it is found that the mean growing spaces are

$$\bar{S}_s = \frac{k}{kN_s + N_a} , \quad \bar{S}_a = \frac{1}{kN_s + N_a} . \quad (8)$$

It can be verified that this agrees with de Wit’s equations, which are expressed in relative terms:

$$S_s = \frac{kP_s}{1 + (k-1)P_s} , \quad S_a = \frac{k^{-1}P_a}{1 + (k^{-1}-1)P_a} .$$

2.3.2. Complementarity

The above assumes a fixed amount of resources per unit area shared between the two cohorts. However, deviations are possible in species mixtures. For instance, different rooting depths can make more soil resources available (Kelty, 1992). Various facilitation and other mechanisms with similar effects can be active and difficult to separate, and are often collectively described as *complementarity* (Forrester, 2014). We model these by increasing (or decreasing) the growing space or resource availability represented on the right-hand side of eq. (7).

A simple modification of eq. (7) might add a term proportional to $4P_s P_a$ to the right-hand side. This is 0 for a single-species stand, and reaches a maximum value of 1 when $P_s = P_a = 1/2$. A slightly more complex form that reflects the species relative crowding was used:

$$4 \left(\frac{kP_s}{kP_s + P_a} \right) \left(\frac{P_a}{kP_s + P_a} \right) = \frac{4kN_s N_a}{(kN_s + N_a)^2}. \quad (9)$$

The maximum is now at $kP_s = P_a$ or $kN_s = N_a$, which corresponds to equal growing spaces: $S_s = N_s \bar{S}_s = N_s k \bar{S}_a = N_a \bar{S}_a = S_a$. Eq. (7) becomes

$$N_s \bar{S}_s + N_a \bar{S}_a = R, \quad (10)$$

with

$$R = 1 + c \frac{4kN_s N_a}{(kN_s + N_a)^2}, \quad (11)$$

c being a *complementarity parameter*. A power of eq. (9) with the exponent as an additional shape parameter could provide additional flexibility, but would likely lead to over-parametrization with our data.

Solving the linear system formed by equations (6) and (10) gives a generalization of de Wit's eq. (8), where the right-hand sides are multiplied by R from eq. (11). Complementarity can be assessed by testing the hypothesis $c = 0$.

2.3.3. Size effects

As noted by de Wit (1960, Ch. 8), the crowding coefficient can be sufficient for characterizing final yields, but at intermediate times the model is strictly valid only if the growth curves are proportional (see also de Wit and van den Bergh, 1965; Firbank and Watkinson, 1985). Cohort size differences become important if these vary substantially over time, as can be expected from the dynamics of competition. Regeneration lags can accentuate size differences (Kabzems and García, 2004).

A simple mechanistic individual-based model was used to derive a plausible functional form for the effects of size. It is based on two ideas:

1. Trees exert a competitive pressure on available resources depending on species, size, and distance. Assume that the pressure (or *influence function*) is proportional to the height of a paraboloid of revolution anchored at the top of the tree, and that at each point in the plane the resource is captured by the tree with the highest influence (Fig. 3). The TASS model of Mitchell (1975) is based on a similar concept, viewing the influence profiles as physical crowns subject to mechanical neighbor interference. Gates et al. (1979) found, given some plausible premises, that the crown profile should be a power function, and that the parabolic case produces polygonal tessellations like those often used in forest growth models (Fig. 3a). The profile can be interpreted more generally as competitive strength, or as a shading potential that can extend beyond the crown surface (García, 2014a). One can relax slightly the assumption by allowing deformations due to neighborhood interactions, provided that the profile cross-sectional area for a tree of height H_i at a level $z \leq H_i$ is proportional to the distance from the top, $b_i(H_i - z)$, where b_i is a species-dependent proportionality constant.
2. The *perfect plasticity approximation* (PPA) postulates that tree crowns are displaced horizontally by stem leaning and by differential branch growth so as to balance competitive pressure on all sides (Strigul et al., 2008; García, 2014b)

These two assumptions imply that the individual growing spaces fill the plane at a certain closure level z^* (Fig. 3b).

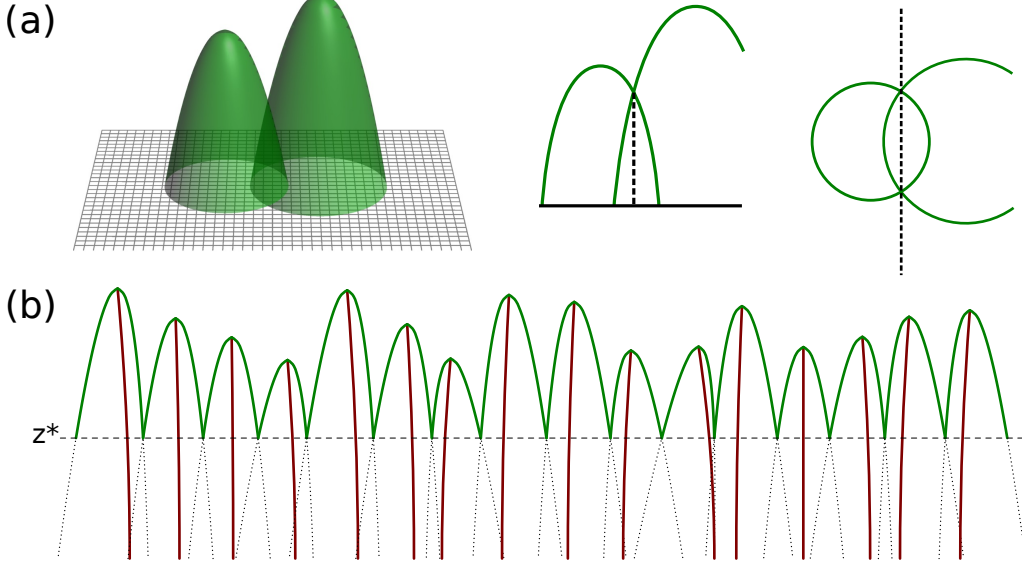


Figure 3: (a) Parabolic crown profiles or influence functions intersect on a polygonal tessellation (after Gates et al., 1979). (b) The perfect plasticity approximation assumes that inter-tree competition intensity is balanced.

Averaging over the spruce and aspen trees, the cohort mean growing space is

$$\bar{S}_s = b_s(\bar{H}_s - z^*), \quad \bar{S}_a = b_a(\bar{H}_a - z^*). \quad (12)$$

Solving the second equation for z^* and substituting into the first,

$$\bar{S}_s = (b_s/b_a)\bar{S}_a + b_s(\bar{H}_s - \bar{H}_a). \quad (13)$$

For the special case of equal heights this coincides with eq. (6), writing $b_s/b_a = k$. Writing also $b_a \equiv b$, the solution of the linear system formed by equations 13 and 10 is:

$$\bar{S}_s = \frac{k}{kN_s + N_a} \left[1 + bN_a(\bar{H}_s - \bar{H}_a) + c \frac{4kN_sN_a}{(kN_s + N_a)^2} \right] \quad (14a)$$

$$\bar{S}_a = \frac{1}{kN_s + N_a} \left[1 + bN_s(\bar{H}_a - \bar{H}_s) + c \frac{4kN_sN_a}{(kN_s + N_a)^2} \right]. \quad (14b)$$

If the calculated space is negative it must be set to 0, indicating complete suppression by the dominant cohort.

In open-canopy stands the calculations above can result in a negative z^* . Setting $z^* = 0$ in those cases would make the total growing space smaller than R , reflecting the less than full site occupancy (Nance et al., 1988). It was preferred, however, to take z^* as a potential closure level and to model occupancy through the Ω state variables of the single-species models.

Parabolic crown or influence profiles generate a polygonal tessellation with growing spaces linear on tree height. Some research suggests, however, that conical profiles with space proportional to $(H_i - z^*)^2$ might be more realistic (García, 2014b; Lee and García, 2016). In that case it

is not possible to obtain simple exact results analogous to equations (13) and (14), but these can still be valid as a first-order approximation. Appendix A extends the results to other profiles and to any number of cohorts. Those cohorts can correspond to different species, or to age or size classes within a same species for modelling uneven-aged stands.

2.4. Heights

2.4.1. Top vs. mean height

Top height is convenient in pure even-aged stands because its development can be predicted with a simple density-independent sub-model, and because it relates to a useful measure of site quality, site index. In complex stands, however, an operational definition of top height is problematic (Zingg, 1994). It is probably best then to consider a cohort top height as a variable that is not directly observable, pertaining to a hypothetical pure stand of the same species, age, and site quality. Therefore, the top height used in the single-species models is linked here to the cohort mean height and mean growing space.

Data from essentially pure spruce and aspen stands were used to obtain relationships between top height H , mean height \bar{H} , and mean growing space \bar{S} . Given the small sample sizes, a much larger data set from loblolly pine plantations was also used to guide the selection of suitable equation forms. Details are shown in Appendix B. The following equations were obtained:

$$H_s/\bar{H}_s = \exp \left[0.10439 \max \left\{ -\ln(150\bar{S}_s), 0 \right\}^{1.159} \right] \quad (\text{spruce}), \quad (15a)$$

$$H_a/\bar{H}_a = \exp \left[0.04732 \max \left\{ -\ln(150\bar{S}_a), 0 \right\}^{1.438} \right] \quad (\text{aspen}). \quad (15b)$$

These can be used for estimating H from \bar{H} , or vice-versa.

2.4.2. Height growth suppression

In multi-layered mixtures it is often observed that the height growth of the dominated species is reduced in relation to that expected in a monoculture (e. g., Kabzems et al., 2016). More generally, a similar suppression of shorter by taller cohorts can occur in uneven-aged stands, or among trees in individual-based models. An initial model version ignoring this did not provide good predictions for some stands, and therefore a height suppression element was introduced.

Height growth suppression is commonly modelled as the product of a “potential” height growth rate and a “modifier” that depends on competitive pressure (Salas et al., 2008; Weiskittel et al., 2011a, Sec. 6.3.1). Here the potential top height growth predicted by eq. (1a) was reduced by a factor determined by the other species density and by the difference in top heights. These are the same variables affecting the growing space in eq. (14). The description that follows is for the usual case where spruce has the smallest height. The opposite situation is rare in our data (Table 1), but for completeness the analogous relationship with the cohort roles reversed was incorporated into the final model.

The spruce height growth reduction must increase with N_a and with $H_a - H_s \equiv \Delta H$, being null if $N_a = 0$ or $\Delta H \leq 0$. Once the spruce is below the base of the aspen canopy there should be no further reduction, that is, an asymptote for increasing ΔH would be expected. It makes sense also for the reduction to be asymptotic in N_a . This can be achieved with a reduction factor (modifier) of the form

$$1 - \alpha F_1(N_a) F_2(\Delta H),$$

where F_1 and F_2 are growth functions with origin 0 and asymptote 1 (or cumulative distribution functions of non-negative variables), and α is a parameter determining the maximum reduction factor $1 - \alpha$. Salas et al. (2008) used a related approach for individual trees.

For a reasonably simple expression one may choose F_1 and F_2 as Hossfeld IV functions:

$$F(x) = \frac{x^\gamma}{x^\gamma + \beta^\gamma} = 1/[1 + (\beta/x)^\gamma]$$

if $x \geq 0$ or 0 otherwise, with β and γ being positive parameters (García, 2008). If over-parametrization due to limited data is a concern, this may be simplified further by fixing γ at a suitable value. Experimentation showed $\gamma = 4$ to be near-optimal, producing a plausible sigmoid shape.

The spruce modifier is then

$$1 - \frac{\alpha}{[1 + (\beta_1/N_a)^{\gamma_1}][1 + (\beta_2/\Delta H)^{\gamma_2}]}, \quad (16)$$

or 1 if $N_a = 0$ or $\Delta H \leq 0$. As mentioned above, the same equation form was used for the aspen height growth modifier, substituting N_s for N_a and $-\Delta H$ for ΔH .

2.5. Parameter estimation

The model parameters to be estimated are k , b and c from eq. (14), α , β_1 and β_2 (and possibly γ_1 and γ_2) from eq. (16), and the localization parameter λ (Sec. 2.2). These were obtained through model projections for interval data (Gadow and Hui, 1999), specifically, from periodic annual increment (PAI) residuals over pairs of consecutive measurements. García (2011, 2013) compared this and other estimation strategies, and found only minor differences in the resulting model predictions. At each measurement the state of the stand was characterized by the mean height, density, and basal area per hectare for each species, i. e., by a vector $(\bar{H}_s, \bar{H}_a, N_s, N_a, B_s, B_a)$. The stands in the database are unthinned and are expected to have reached full or nearly full canopy closure, so that for estimation the occupancy factor was fixed at $\Omega_s = \Omega_a = 1$.

The model has a hierarchical aspect, involving also site quality parameters q specific to each stand and cohort. These are functionally related to conventional site indices through the integral of eq. (1a) at some reference age. More generally, q can vary over time, reflecting climate variability and the effect of pests (Fontes et al., 2010). An initial model version computed q -values for each measurement interval from the observed heights and densities, effectively eliminating the time variable by expressing basal area growth and mortality relative to height growth (García, 2013). Introduction of height growth suppression, however, required a more complex two-stage approach: at each iteration, q was first estimated for each plot minimizing squared height residuals, and then used in the current parameter estimation step. The spruce q_s and aspen q_a were constrained to satisfy

$$\text{Spruce Site Index} = 3.804 + 0.7978 \times \text{Aspen Site Index} \quad (17)$$

(Nigh, 2002).

Fitting was performed based on residuals of basal area and of the logarithm of stand density. The logarithm $\ln N$ was preferred to N because it makes the residuals more symmetric and homoscedastic. Parameter values affect jointly basal area growth and mortality, and these variables can be expected to be correlated, so that this is a multiresponse parameter estimation problem

(Box and Draper, 1965; Bates and Watts, 1985; García, 1988; Seber and Wild, 2003, Ch. 11). Based on a Bayesian analysis, Box and Draper (1965) recommended minimizing the determinant of the residual sum of squares matrix. The same criterion was obtained by Bard (1974, Sec. 4–9) as the maximum likelihood estimator under the usual normality assumptions. As shown by Seber and Wild (2003), it is equivalent to quasi-maximum-likelihood or generalized least-squares estimation in more general distribution-free settings. Several methods of approximate computation have been proposed (Bates and Watts, 1985; Seber and Wild, 2003, Ch. 11). However, with modern computing power, direct numerical optimization of the Box-Draper criterion with general-purpose software has become feasible. Parameter estimates were calculated using the `optim` R function (R Development Core Team, 2009) to minimize the logarithm of the determinant of the 6×6 sum of squares matrix of PAI residuals for H_s , H_a , $\ln N_s$, $\ln N_a$, B_s and B_a .

It is interesting to test statistically for complementarity effects, that is, to test if c is significantly different from 0. A likelihood ratio test suggested by Seber and Wild (2003, p. 538) was used. It is based on the determinant of the sum of squares matrix for the full model, $|\hat{V}|$, and that for the model with $c = 0$, $|\hat{V}_0|$. Under the null hypothesis $c = 0$ and with a sample of n observations, $n(\ln |\hat{V}| - \ln |\hat{V}_0|)$ has asymptotically a chi-squared distribution with 1 degree of freedom. The likelihood ratio was useful also for testing significance of localization and other parameters.

For the residual computations, state projections from the start to the end of a measurement interval were performed as follows. First, q_s and q_a values were obtained as explained above, and initial top heights H_s, H_a were calculated from the mean heights and densities with equations (14) and (15). These heights were used to compute the initial state vector

$$(H_s, H_a, \ln N_s, \ln N_a, \bar{W}_s, \bar{W}_a)$$

in the system of differential equations (1a), (2a), (2b). The differential system was integrated numerically from the initial to the final interval time with function `ode` of the `deSolve` R package (Soetaert et al., 2010). At each step, equations (14) and (15) have to be solved-back numerically for \bar{S}_s and \bar{S}_a . Finally, the projected mean heights, densities and basal areas $B = \bar{W}N/H$ are extracted from the integration output. Section 3.2 gives a summary of the projection procedure.

Full computational details and computer code are included in the Supplementary Material.

3. Results

3.1. Estimates

A number of optimization runs were performed, with and without c , λ , or height growth suppression, with various values for γ , and using the Nelder and Mead or the BFGS options of `optim`. Different starting points were used to guard against local optima. Results were consistent, with typical run times, starting from rough initial estimates, of 20 to 40 minutes on a modern personal computer.

Accounting for height growth suppression was clearly necessary. Fixing γ at 4 was better than at 2 or 3, although the differences were not statistically significant. Leaving γ_s and γ_a as free parameters did not produce any appreciable improvement. The final parameter estimates (with $\gamma_s = \gamma_a = 4$) are given in Table 4, together with approximate standard errors. The standard errors are based on the observed information matrix given by the inverse Hessian of the optimized log-likelihood (Efron and Hinkley, 1978; Seber and Wild, 2003; Venables and Ripley, 2002, Sec. 16.3).

Table 4: Parameter estimates.

Parameter	Estimate	Standard error
k	1.317	0.0669
b	0.2153×10^{-4}	0.0460×10^{-4}
c	0.2078	0.0623
α	0.2876	0.0316
β_1	33.81	50.5
β_2	3.459	0.609
λ	1.448	0.0483

The higher competitive strength of spruce relative to aspen implied by the relative crowding coefficient $k = 1.317$ agrees with the similar, although higher value $6.543/3.663 = 1.786$ found by Lee and García (2016) in spruce-hardwood mixedwoods. The complementarity parameter c was significantly different from 0 ($p = 8.2 \times 10^{-11}$), giving a maximum growing-space gain of 21% for mixtures relative to monocultures (eq. (11)). The aspen localization parameter λ was significantly different from 1 ($p = 9.0 \times 10^{-10}$), indicating larger diameters for a common height in British Columbia compared to the predictions of the western Canada model. A similar λ was obtained using only pure-aspen plots.

Figure 4 shows the basal area and mortality residuals, related to species composition. The residual is the difference between the observed and predicted PAI, i. e., the difference of the values at the second measurement of the interval pair divided by the interval length. Spruce basal area percentages are ratio-of-means averages for the interval.

3.2. Model summary and implementation

At any point in time the stand can be described by the 8 state variables $\bar{H}_s, \bar{H}_a, N_s, N_a, B_s, B_a, \Omega_s, \Omega_a$. The growth model predicts the change of state between any two times. That is done by numerically integrating a system of differential equations.

To simplify, it is convenient to write those differential equations in terms of alternative state variables from Sect. 2.2. New values for the original state can be recovered after the integration. Specifically, we use the “mean bulk” $\bar{W}_s = B_s H_s / N_s$ and $\bar{W}_a = B_a H_a / N_a$, and the top heights H_s and H_a given by

$$H_s = \bar{H}_s \exp \left[0.10439 \max \left\{ -\ln(150\bar{S}_s), 0 \right\}^{1.159} \right] \quad (18a)$$

$$H_a = \bar{H}_a \exp \left[0.04732 \max \left\{ -\ln(150\bar{S}_a), 0 \right\}^{1.438} \right] \quad (18b)$$

(c. f. eq. (15)). Some of the numerical coefficients derived from parameter estimates are given below at full precision to prevent rounding artifacts.

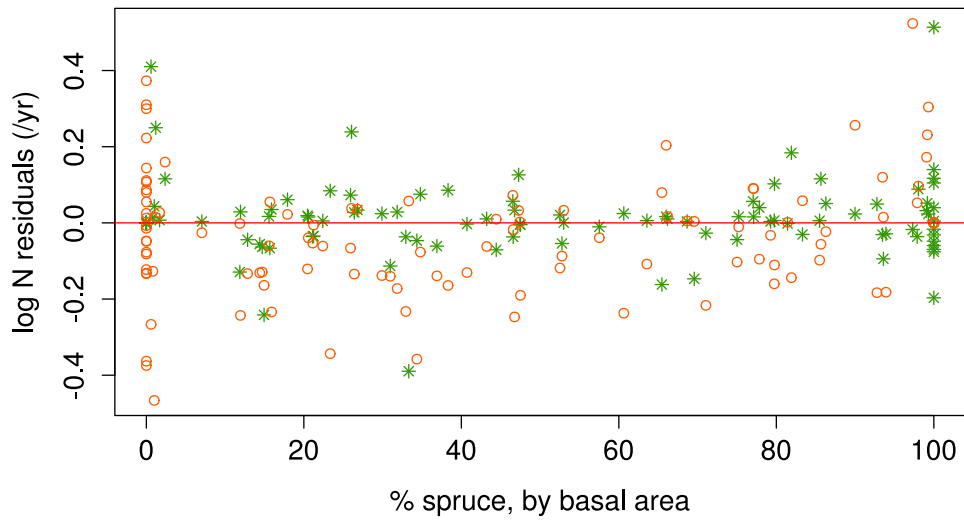
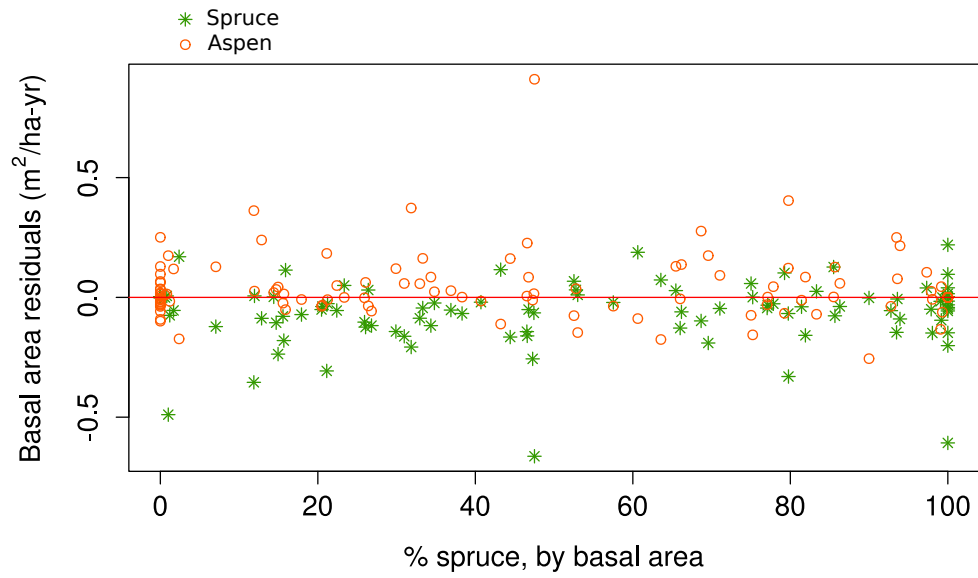


Figure 4: Measurement interval periodic annual increment residuals (see text).

From eq. (14), the mean growing space \bar{S}_s and \bar{S}_a is

$$\bar{S}_s = \max \left\{ \frac{1.317}{1.317N_s + N_a} \left[1 + 0.00002153N_a(\bar{H}_s - \bar{H}_a) + 1.09469 \frac{N_s N_a}{(1.317N_s + N_a)^2} \right], 0 \right\} \quad (19a)$$

$$\bar{S}_a = \max \left\{ \frac{1}{1.317N_s + N_a} \left[1 + 0.00002153N_s(\bar{H}_a - \bar{H}_s) + 1.09469 \frac{N_s N_a}{(1.317N_s + N_a)^2} \right], 0 \right\}. \quad (19b)$$

After integration, iterative numerical methods are needed to solve these relationships for the original variables.

Substituting parameter values in equations (1a) and (2), and using eq. (16) and the aspen localization, the state transitions are given by the following system of differential equations:

$$\frac{dH_s}{dt} = (q_s/0.5829)H_s \left[\left(283.87q_s^{0.5137}/H_s \right)^{0.5829} - 1 \right] \left\{ 1 - \frac{0.4229(N_a \max\{H_a - H_s, 0\})^4}{(N_a^4 + 883667)[(H_a - H_s)^4 + 178.073]} \right\} \quad (20a)$$

$$\frac{dH_a}{dt} = q_a H_a [(8.568 + 1342q_a)/H_a - 1] \left\{ 1 - \frac{0.4229(N_s \max\{H_s - H_a, 0\})^4}{(N_s^4 + 883667)[(H_s - H_a)^4 + 178.073]} \right\} \quad (20b)$$

$$\frac{d \ln N_s}{dt} = - \left(4.5759 \times 10^{-15} H_s^{5.009} / \bar{S}_s^{1.9895} \right) \frac{dH_s}{dt} \quad (20c)$$

$$\frac{d \ln N_a}{dt} = - \left(0.000690992 / \bar{S}_a^{0.6159} \right) \frac{dH_a}{dt} \quad (20d)$$

$$\frac{d\bar{W}_s}{dt} = 0.5345\Omega H_s \bar{S}_s^{0.7} \frac{dH_s}{dt} - 0.7\bar{W}_s \frac{d \ln N_s}{dt} \quad (20e)$$

$$\frac{d\bar{W}_a}{dt} = 1.29684\Omega H_a \bar{S}_a^{0.7971} \frac{dH_a}{dt} - 0.5\bar{W}_a \frac{d \ln N_a}{dt} \quad (20f)$$

with

$$\Omega_s = 1 - (1 - \Omega_{0s}) \exp \left[-0.0258214(H_s^2 - H_{0s}^2) \right] \quad (21a)$$

$$\Omega_a = 1 - (1 - \Omega_{0a}) \exp \left[-0.015(H_a^2 - H_{0a}^2) \right], \quad (21b)$$

where $H_{0s}, H_{0a}, \Omega_{0s}, \Omega_{0a}$ are values at the initial time.

The truncation at 0 in eq. (19) and in other functions produces a slope discontinuity that could cause numerical difficulties in optimization or zero-finding algorithms. Therefore, a smooth strictly positive hyperbolic approximation was substituted for the bound in those instances:

$$\max\{x, 0\} \approx \frac{1}{2} \left(x + \sqrt{x^2 + \epsilon^2} \right). \quad (22)$$

The largest discrepancy is $\epsilon/2$ at $x = 0$. For a good approximation this tolerance should be small enough to be practically negligible, but not so small as to generate numerical underflows. An ϵ

close to the mean of x times 10^{-4} seems adequate in most cases. A smoother transition obtained with larger values of ϵ might however be more realistic.

In addition to the R functions used in model fitting, SAM has been implemented as an easy-to-use interactive simulator. The simulator, using Microsoft Excel with Visual Basic macros, was based on those of García (2011, 2013) and García et al. (2011), and it is available in the Supplementary Material.

Avoiding numerical integration of the Ω 's in the simulator was important, because these are fast variables that produce stiff differential equation systems, requiring sophisticated adaptive algorithms for accurate solutions (e. g., Soetaert et al., 2010). Making use of eq. (21), a relatively simple modified 4th-order Runge-Kutta method with fixed time-step was sufficient. Careful debugging to achieve consistency of results among the simulator, the R functions, and the single-species models, makes serious programming errors unlikely.

The SAM simulator produces tables of state variables, yields and other outputs for any sequence of times starting from a given state. By default, initial states at stand establishment are generated by the methods described in Appendix C, including an optional spruce regeneration lag. Disturbances can be simulated at any time by introducing arbitrary changes in the state variables.

Appendix D derives total volume functions based on SAM's state variables. These, and merchantable volume relationships from Scube and TAG, are used to calculate stand volumes to any merchantability index given the current state variables. Other outputs like carbon or biomass can be easily added. Facilities are also provided to derive site quality from conventional site indices, optionally enforcing the species site equivalence of eq. (17).

3.3. Examples

Three examples are given to illustrate potential uses of the SAM simulator in some research and management problems, and to examine model behavior.

3.3.1. Replacement diagrams

Replacement diagrams or replacement series experiments were popularized by de Wit (1960) for studying plant competition or interference effects in two-species mixtures (e.g., Harper, 1977; Kilty, 1992; Jolliffe, 2000; Condés et al., 2013; Forrester and Pretzsch, 2015). The diagram plots some measure of yield for each component and for the total of the mixture as functions of species composition, maintaining a constant total density. The original application of de Wit (1960) deals with seed yields at harvest in an annual crop, and both yields and composition are in terms of number of seeds per unit area. The situation is less clear in perennials (de Wit and van den Bergh, 1965; Firbank and Watkinson, 1985), and in forests in particular a variety of yield and species composition measures have been proposed (Dirnberger and Sterba, 2014; Sterba et al., 2014). In addition to the density level, a harvest age has to be chosen.

For illustration purposes, an initial density of 5000 trees/ha (at breast height) and a harvest age of 100 years were specified. Spruce site index was 18, with the default 17.79 for aspen according to eq. (17). The default initialization procedure with spruce regeneration by planting was used (Appendix C). Total volumes per hectare were computed with the SAM simulator for initial spruce numbers of 0, 10%, 20%, ..., 100%, but plotted over the more commonly used species composition % by basal area. The result is shown in Fig. 5. The customary straight lines drawn for comparison indicate the expected relationships in the absence of interactions, e. g., on side-by-side monocultures.

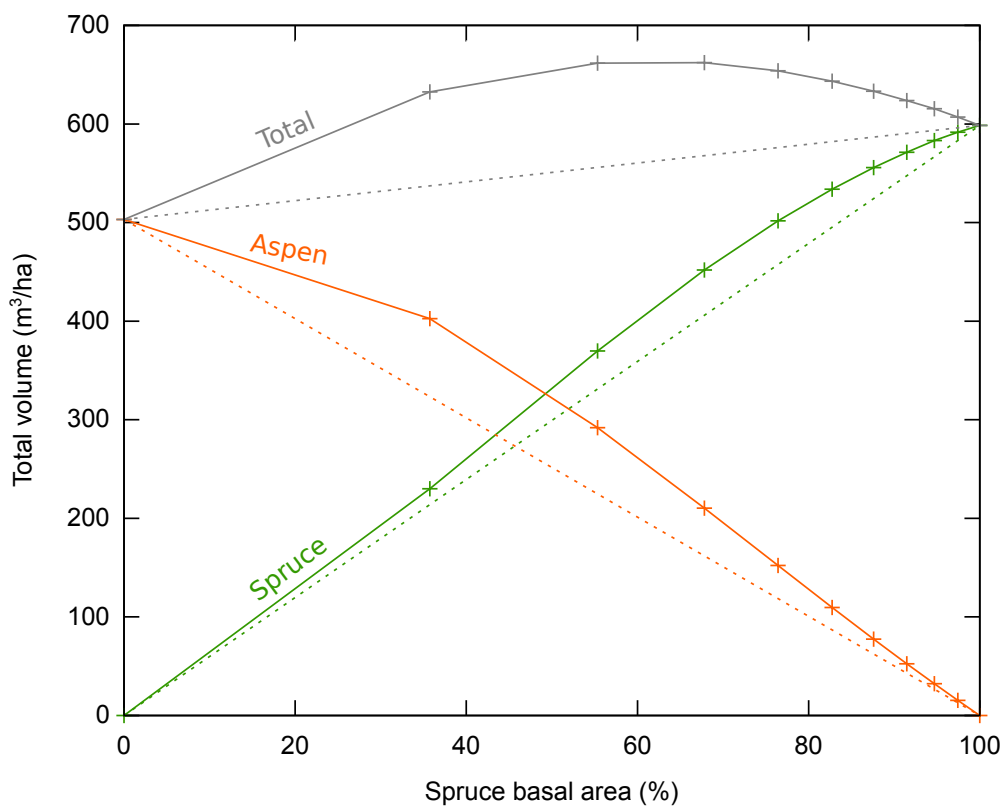


Figure 5: Replacement diagram for age 100 years, 5000 trees/ha initial density, spruce site index 18. The dashed straight lines correspond to no interaction.

The Figure is similar to typical replacement diagrams found in the literature. It exhibits higher yields in mixture than in monoculture, commonly termed *overyielding*.

3.3.2. Optimization

As pointed out, among others, by Firbank and Watkinson (1985), Jolliffe (2000), and Lilles and Coates (2014), replacement series and other mixture experiments are often difficult to interpret because of confounding with stand density and other factors. The yield criterion may or may not represent management objectives and costs, and the best harvesting age may differ among the monocultures and the mixture. Moreover, basal area or other composition indicators are largely responses and not management decision variables. Growth models can provide more flexible means for addressing these issues (Firbank and Watkinson, 1985).

With SAM it is not difficult to choose management variables in a more realistic setting. The Excel *Solver* facility can be used to compute their optimal values. As a simple example, it is shown how to maximize long-term CO₂ sequestration in timber production. We consider only long term off-site carbon storage in forest products (McKinley et al., 2011).

Merchantable volume per hectare to a merchantability limit of 15 cm was multiplied by basic density, 0.35 and 0.37 for spruce and aspen, respectively, to obtain wood production in metric tonnes per hectare (Forest Products Laboratory, 1999, Table 4a). Carbon wood content is normally between 0.48 and 0.50, which can be multiplied by 44/12 to convert to CO₂ units. Dividing by the harvesting age gives a spreadsheet entry for mean annual CO₂ sequestering in tons/ha-yr, which is selected in the Solver as the objective to be maximized.

Site indices and initialization were as in the previous example, except for the initial densities. The 3 decision variables in the Solver were the initial numbers of trees per hectare for spruce and aspen, and the harvest age. Runs for monocultures were also performed, fixing the initial density at 0 for one of the two cohorts. Optimization takes a fraction of a second, and gave the results in Table 5.

Table 5: Maximizing carbon sequestration

Composition	CO ₂ (T/ha-yr)	Rotation (yr)	Initial spruce / ha	Initial aspen / ha
Mixture	3.778	106.9	1573	6398
Spruce	3.729	94.1	892385	0
Aspen	2.872	83.5	0	1782

Optimization is a stringent test, being “remarkably efficient at exploiting seemingly minor quirks in models to arrive at unrealistic solutions” (Vanclay and Skovsgaard, 1997). That was the case for initial density in the spruce monoculture.

3.3.3. Spruce regeneration lags

Delays in the regeneration of a cohort can have important consequences for stand dynamics. In particular, spruce regeneration lags after a stand-replacing fire can produce distinct dominance patterns, which can be mistaken by chronosequence stages in the so-called classical dynamics successional pathway (Kabzems and García, 2004; Johnson and Miyanishi, 2008; Bergeron et al., 2014). The SAM simulator implements a spruce regeneration delay that can be used to study these issues.

Figure 6 shows simulated mean heights and diameters with a 40-yr spruce regeneration lag, compared to projections without a lag. Site indices were 19 and 21, and initial densities 1000

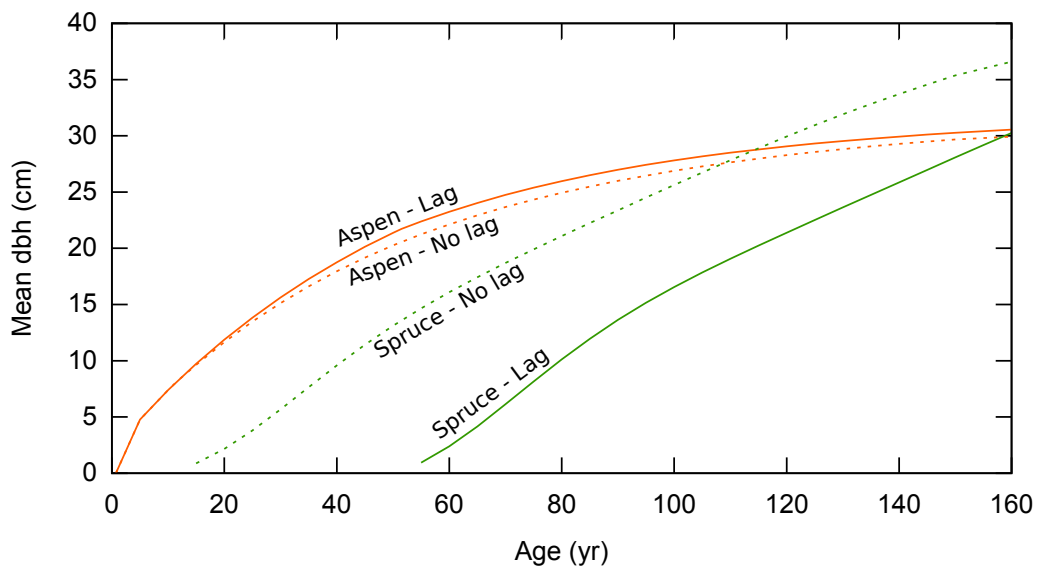
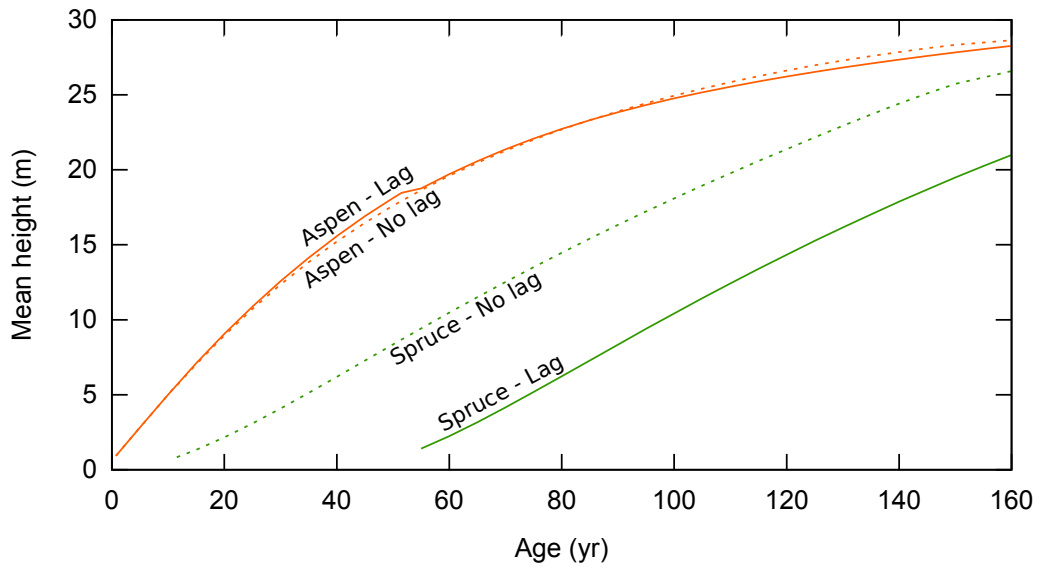


Figure 6: Simulated mean height and mean diameter trends with and without a spruce regeneration lag (c. f. Kabzems and García (2004)).

and 8000 trees / ha, for spruce and aspen, respectively. Mean height and diameter trends are qualitatively similar to those reconstructed through stem analysis by Kabzems and García (2004), although the lag effects appear somewhat smaller than suggested by that study.

4. Discussion and Conclusions

The process of data preparation and preliminary analysis pointed to some interesting patterns. The breakup often reported in mature aspen stands (Frey et al., 2004) was not evident in our data from British Columbia. Aspen diameters and basal area for any given height tended to be higher than those predicted by the TAG model for the whole of western Canada, an observation confirmed by a statistically significant localization parameter. Kabzems and García (2004) commented on the large size of individual trees, longevity, and the low occurrence of internal decay in trembling aspen in northeastern British Columbia compared to other boreal forests. To some extent this may apply to the rest of the Province, although biogeoclimatic zone comparisons with the available data are inconclusive.

On the other hand, there were clear indications of heavy mortality among older spruce trees. Such spruce old-growth stand breakup does not seem to have been previously reported in the literature. If confirmed, it can have important implications for sustainable forest management and wood supply, so that further research on this matter is desirable.

It is worth mentioning also the effectiveness of the ingrowth imputation procedure. Similar methods can avoid awkward ingrowth modelling problems, and make better use of young stand data whenever trees are not measured below some size threshold, a common practice in natural forests.

Current individual-based methods present problems with emergent properties and statistical confounding that have not yet been generally recognized. These issues deserve attention, given the undeniable value of those methods for studying the ecological fundamentals of stand dynamics. Meanwhile, aggregation has the potential for side-stepping some of those difficulties and providing adequate management tools, even if only as a stop-gap measure. However, although aggregation reduces the number of variables, it increases the level of abstraction, making less obvious the mapping between modelling elements and the real world compared to the typical individual-tree model. That has hampered the development of mechanistic aggregate stand-level models for other than single-species even-aged stands. This work is a preliminary exploration of a conceptual framework and methods for modelling complex stands at the stand level.

Turning to the model components, already available single-species models served as a starting point, linking the cohort models through space partitioning relationships. In other situations, the single-species models would need to be developed from scratch, possibly helped by the perfect plasticity theory from section 2.3.3, as outlined on p. 11 of García (2014b). In any case, when there is a need for predictions beyond the environmental and management conditions represented in the available data, one should avoid the common practice of using stem thickness measures such as diameter or basal area as driving variables (García et al., 2011; Lee and García, 2016)

Resource capture or growing space is a highly simplified abstraction of ecological processes, but it seems a useful basis for modelling and understanding interactions in forest stands (Monteith, 1994). The space partitioning model of de Wit (1960) was extended to deal with distinct tree sizes, and to allow for differences in resource use efficiency between mixtures and monocultures (complementarity). In the spruce-aspen stands, de Wit's relative crowding coefficient of

spruce with respect to aspen was estimated as $k = 1.317$, with a statistically significant difference from 1, indicating that spruce trees capture more site resources than equally tall aspens. The term accounting for the effect of tree height differences was also significant, with substantially more space allocated to taller cohorts. There was support for enhanced efficiency in spruce-aspen mixtures, with a statistically significant estimated increase of up to 21% in resource availability relative to monocultures. The space allocation model makes possible an objective testing of theoretical arguments and assumptions common in the literature.

Mean cohort heights, suitable as mixture state variables, could be related satisfactorily to stand density and the more convenient top heights used in single-species even-aged models. Relationships similar to those developed in Appendix B would be useful in other forestry applications. Including height growth suppression complicated substantially the model structure and parameter estimation, but it clearly improved predictions in the more highly stratified plots. It was necessary for approximating the observed behavior under regeneration lags described in Sec. 3.3.3.

Parameter estimation in this model is unusually complex. It involves multiresponse, with panel data, in a hierarchical model constituted by a system of nonlinear differential equations that need to be numerically integrated. Each evaluation requires also iterative root finding. With common distributional assumptions, minimizing the Box-Draper multiresponse determinant criterion corresponds to maximum likelihood or Bayesian estimation, and it has the good asymptotic properties of generalized least-squares under less restrictive conditions. It is an interesting reflection on modern computing power that estimates could be obtained with standard numerical analysis software on a personal computer, in a reasonable amount of time and without major difficulties. Satisfactory fits were verified by analysis of residuals, parameter statistics and simulations

The spruce-aspen simulator demonstrates a user-friendly and flexible implementation. Most users are already familiar with spreadsheet software, and the complexity of the calculations is hidden in efficiently coded macros that execute quickly in the background. Besides showing the model's plausible behavior, the examples of Sect. 3.3 suggest the nature of possible applications. In particular, built-in optimization tools can easily answer questions that until recently would have been regarded as sizable research projects.

SAM, the spruce-aspen model, must be viewed largely as an experiment for testing the methodology. Still, it can be useful for management planning and for guiding research if its limitations are kept in mind. Suitable data from mixed stands was rather scarce, and the model would benefit from further testing with new experimental data that is gradually becoming available (e. g., Bokalo et al., 2007; Gradowski et al., 2008; Comeau et al., 2009; Kabzems et al., 2016). SAM is not expected to be reliable in old-growth stands due to the unpredictability of die-back in mature aspen (Frey et al., 2004; Hogg et al., 2008; Worrall et al., 2013), and possibly in older spruce (Sec. 2.1). Reliability is also uncertain in early stand development, where competition or facilitation mechanisms and relationships may differ from those in older stands, and where the effects of understory vegetation can be important. In some instances, a third cohort for the herbaceous vegetation might better reflect the interactions (Cosmin et al., 2008). The general approach, however, seems useful as a basis for future work with these and other species or stand types.

Acknowledgements

The data were provided by the Forest Analysis and Inventory Branch of the B. C. Ministry of Forests, Lands and Natural Resource Operations, and I am particularly grateful to Rene De Jong

and Pat Martin for help in data extraction and interpretation. Thanks also to the Virginia Tech Forest Modeling Research Cooperative for permission to use the loblolly pine data in Appendix B. Comments from anonymous referees contributed to improve the text.

Appendix A. Growing space partitioning

This appendix extends the relationships of Section 2.3.3 to any number of cohorts and to other than parabolic profiles.

Let the growing space or resource captured by tree i in cohort j be

$$S_{ij} = b_j(H_{ij} - z^*)^\theta, \quad (\text{A.1})$$

where H_{ij} is the tree height, z^* is the closure level, and b_j and θ are positive parameters (Fig. 3). This assumes that $H_{ij} \geq z^*$, otherwise the tree is completely over-topped and does not receive any resources. Any such trees are excluded from the calculations that follow, which might require some iterations since z^* is not known in advance.

The cohort means are

$$\bar{S}_j = b_j \overline{(H_{ij} - z^*)^\theta}, \quad (\text{A.2})$$

with the overline indicating a mean over the trees in cohort j . The level z^* can be obtained from the fact that, with full closure (i. e., $z^* \geq 0$), the individual values add up to the total available resource R :

$$\sum_{ij} S_{ij} = \sum_j N_j \bar{S}_j = R.$$

In what follows, the number of trees N_j and R are quantities per unit area. Therefore,

$$\sum_j N_j b_j \overline{(H_{ij} - z^*)^\theta} = R. \quad (\text{A.3})$$

This equation can be solved for z^* , generally by numerical methods.

If z^* is found to be negative, it can be taken as defining a potential resource capture, using then other means for modelling stand openness, as in SAM. Alternatively, z^* can be bound at 0, giving a less than full site occupancy in eq. (A.2):

$$\bar{S}_j = b_j \overline{H_{ij}^\theta}. \quad (\text{A.4})$$

The approximation in eq. (22) could be used to preserve smoothness.

Explicit results can be obtained for $\theta = 1$ and for $\theta = 2$.

Case $\theta = 1$

Eq. (A.2) becomes

$$\bar{S}_j = b_j(\bar{H}_j - z^*), \quad (\text{A.5})$$

and from eq. (A.3),

$$\sum_j N_j b_j \bar{H}_j - z^* \sum_j N_j b_j = R,$$

so that

$$z^* = \frac{\sum_j N_j b_j \bar{H}_j - R}{\sum_j N_j b_j}. \quad (\text{A.6})$$

Case $\theta = 2$

Now eq. (A.2) becomes

$$\bar{S}_j = b_j(\bar{H}_j - z^*)^2, \quad (\text{A.7})$$

and eq. (A.3) is

$$\sum_j N_j b_j \overline{(H_{ij} - z^*)^2} = R.$$

This gives a quadratic equation in z^*

$$(z^*)^2 \sum_j N_j b_j - 2z^* \sum_j N_j b_j \bar{H}_j + \sum_j N_j b_j \bar{H}_{ij}^2 - R = 0 \quad (\text{A.8})$$

that can be analytically solved for z^* .

For a somewhat simpler expression, define \tilde{H} as the weighted mean

$$\tilde{H} = \frac{\sum_j N_j b_j \bar{H}_j}{\sum_j N_j b_j}, \quad (\text{A.9})$$

and

$$\tilde{\sigma}^2 = \frac{\sum_j N_j b_j \tilde{\sigma}_j^2}{\sum_j N_j b_j} = \frac{\sum_j N_j b_j \overline{(H_{ij} - \tilde{H})^2}}{\sum_j N_j b_j}, \quad (\text{A.10})$$

a weighted variance. Then write

$$\begin{aligned} R &= \sum_j N_j b_j \overline{(H_{ij} - z^*)^2} = \sum_j N_j b_j \overline{(H_{ij} - \tilde{H}) + (\tilde{H} - z^*)^2} \\ &= \sum_j N_j b_j [\overline{(H_{ij} - \tilde{H})^2} + (\tilde{H} - z^*)^2] \\ &= [\tilde{\sigma}^2 + (\tilde{H} - z^*)^2] \sum_j N_j b_j \end{aligned}$$

(the cross-products term vanishes). Finally, solving for z^* ,

$$z^* = \tilde{H} - \sqrt{\frac{R}{\sum_j N_j b_j} - \tilde{\sigma}^2}. \quad (\text{A.11})$$

Appendix B. Top height vs. mean height

Measurements with at least 95% of basal area in either spruce or aspen were selected to obtain relationships between top height H , mean height \bar{H} , and trees per hectare N . Given the small size of these samples, a much larger data set from loblolly pine plantations used by García et al. (2011) helped in testing for appropriate equation forms.

Data statistics are shown in Table B.6. Another interesting characteristic is the height variability within plots. The mean coefficient of variation was 22.3% for spruce, 15.8% for aspen, and 9.9% for pine. Heights were estimated from height-diameter regressions in spruce and aspen, but measured directly on all trees in the pine data.

Table B.6: Data for height relationships. Trees per hectare N , and mean height \bar{H} (m).

	Spruce ($n = 26$)		Aspen ($n = 52$)		Pine ($n = 1156$)	
	N	\bar{H}	N	\bar{H}	N	\bar{H}
Mean	1380	13.34	2481	17.34	951	15.37
S. D.	536	7.67	1407	4.75	430	3.74
Min.	568	3.34	338	10.67	253	5.75
Max.	2275	30.94	7075	29.50	2644	26.07

Equations were conditioned to give a top height equal to the mean height at 150 trees / ha, the approximate top trees selection rate $160 - 0.6/A$ for our mean plot size $A = 0.09$ ha (García, 1998). The logarithm of the height ratio $\log(H/\bar{H})$ was used as dependent variable in the regressions, because it gives the same parameter estimates when estimating H from \bar{H} or vice-versa, and because of improved homocedasticity.

Equation forms were screened by comparison to theoretical relationships generated from Weibull distributions, and to the empirical data. Best results were obtained with $\ln(H/\bar{H}) = a(N - 150)^b$, $\ln(H/\bar{H}) = a[\ln(N/150)]^b$, $\ln(H/\bar{H}) = a[(N/150)^b - 1]$, and with $\ln(H/\bar{H}) = a[\sqrt{N/150} - 1]$, all these equations producing very similar fit statistics. The second form was finally chosen, written as

$$\ln(H/\bar{H}) = a \max\{\ln(N/150), 0\}^b \quad (\text{B.1})$$

to include values of $N < 150$. The nonlinear least squares estimates are given in Table B.7. For mixtures, the reciprocal $1/\bar{S}$ of the mean space per tree was substituted for N (eq. (15)).

Table B.7: Nonlinear regressions for eq. (B.1)

Species	n	\hat{a}	\hat{b}	RSE
Spruce	26	0.10439	1.159	0.07265
Aspen	52	0.04732	1.438	0.07685
Pine	1156	0.03466	1.487	0.02746

Appendix C. Simulation initialization

SAM should be most reliable projecting the development of closed-canopy stands starting from a known state. However, it is also interesting to simulate stand dynamics from stand initiation. In the single-species models it was convenient to initialize at breast-height age, but the fact that spruce reaches breast height later than aspen complicates modelling for mixed stands. The effect of lags in spruce regeneration is also important (Kabzems and García, 2004; Bergeron et al., 2014). The implemented simulator provides the following initialization procedure by default, although other options can be used.

An aspen stand is started with a top height of 1.3 m (breast height), a user-supplied number of trees, basal area 0, and occupancy estimated as a function of the number of trees as in Section 3.3.3 of García (2013). The time origin is set at stand initiation, with the time at breast height being

$$-\frac{1}{q} \ln\left(1 - \frac{1.3}{8.568 + 1342q}\right) - 1.183 \quad (\text{C.1})$$

(García, 2013, eq. 5).

Spruce is similarly introduced when it reaches breast height, at time $7.7 + 111/\text{site index}$ for natural seed-origin stands, or $1.7 + 111/\text{site index}$ if the spruce is planted (Hu and García, 2010). A spruce regeneration lag can be added if regeneration does not occur at the time of stand initiation. In this case growing space and mean heights are calculated for the mixture with equations (14) and (15), and the reciprocal of the spruce growing space is used instead of number of trees in the occupancy equations of García (2011). This implies neglecting any effects of spruce on aspen growth before the spruce reaches breast height.

As noted elsewhere, SAM might not represent well seedling development below breast height. Competition, facilitation and complementarity mechanisms can differ among life stages, the empirical single-species occupancy relationships may not be accurate for mixtures, and the presence of secondary vegetation and soil and vegetation control treatments can be important factors. Simulations from stand initiation can be useful, but currently their accuracy is uncertain.

Appendix D. Volume equations

The total volume per hectare V for each species needs to be estimated from the state variables. Table D.8 gives statistics for the measurements available. All measurements containing the target species were used, regardless of mixing proportions.

Table D.8: Data for volume regressions. Mean height \bar{H} (m), basal area B (m^2/ha), and total volume V (m^3/ha).

	Spruce ($n = 401$)			Aspen ($n = 389$)		
	\bar{H}	B	V	\bar{H}	B	V
Mean	16.70	23.88	224.6	18.69	17.59	146.7
S. D.	7.49	15.81	187.0	5.25	13.66	128.4
Min.	3.34	0.02	0.0	6.30	0.07	0.2
Max.	35.05	70.95	904.3	35.13	63.28	789.6

A large number of regressions and weightings were tested through stepwise regression and graphical analysis. Species composition had no appreciable effect, and neither had the inclusion of number of trees or growing space. That left the cohort basal area B and the mean height \bar{H} as suitable predictors. Using the form factor $V/(B\bar{H})$ as dependent variable gave good results, and little improvement was obtained with relationships more complicated than simple linear regressions on \bar{H} . The final models, with the subscripts s and a for spruce and aspen, respectively, were:

$$\frac{V_s}{B_s \bar{H}_s} = 0.5873 - 0.005386 \bar{H}_s, \quad \text{RSE: } 0.07261 \quad (\text{D.1})$$

$$\frac{V_a}{B_a \bar{H}_a} = 0.4765 - 0.002196 \bar{H}_a, \quad \text{RSE: } 0.02894 \quad (\text{D.2})$$

In the simulator, negative values are suppressed as $V/(B\bar{H}) = \max\{b_0 - b_1 \bar{H}, 0\}$, smoothing the transition with eq. (22).

References

Atta-Boateng, J., Moser, Jr., J.W., 2000. A compatible growth and yield model for the management of mixed tropical rain forest. Canadian Journal of Forest Research 30, 311–323.

- Bard, Y., 1974. Nonlinear Parameter Estimation. Academic Press, New York. 341 p.
- Bates, D.M., Watts, D.G., 1985. Multiresponse estimation with special application to linear systems of differential equations. *Technometrics* 27, 329–339.
- Bergeron, Y., Chen, H.Y.H., Kenkel, N.C., Leduc, A.L., Macdonald, S.E., 2014. Boreal mixedwood stand dynamics: Ecological processes underlying multiple pathways. *The Forestry Chronicle* 90, 202–213. doi:10.5558/tfc2014-039.
- Bokalo, M., Comeau, P.G., Titus, S.J., 2007. Early development of tended mixtures of aspen and spruce in western Canadian boreal forests. *Forest Ecology and Management* 242, 175–184.
- Box, G.E.P., Draper, N.R., 1965. The Bayesian estimation of common parameters from several responses. *Biometrika* 52, 355–365.
- Comeau, P.G., Filipescu, C.N., Kabzems, R., DeLong, C., 2009. Growth of white spruce underplanted beneath spaced and unspaced aspen stands in northeastern B.C. — 10 year results. *Forest Ecology and Management* 257, 1087–1094.
- Condés, S., Del Rio, M., Sterba, H., 2013. Mixing effect on volume growth of *Fagus sylvatica* and *Pinus sylvestris* is modulated by stand density. *Forest Ecology and Management* 292, 86–95. doi:10.1016/j.foreco.2012.12.013.
- Cosmin, D.M., Comeau, P.G., Pitt, D.G., 2008. Competitive effects of woody and herbaceous vegetation in a young boreal mixedwood stand. *Canadian Journal of Forest Research* 38, 1817–1828. doi:10.1139/X08-032.
- Dirnberger, G.F., Sterba, H., 2014. A comparison of different methods to estimate species proportions by area in mixed stands. *Forest Systems* 23.
- Efron, B., Hinkley, D.V., 1978. Assessing the accuracy of the maximum likelihood estimator: Observed versus expected Fisher information. *Biometrika* 65, 457–483. doi:10.1093/biomet/65.3.457.
- Firbank, L.G., Watkinson, A.R., 1985. On the analysis of competition within two-species mixtures of plants. *Journal of Applied Ecology* 22, 503–517. doi:10.2307/2403181.
- Flewelling, J.W., de Jong, R., 1994. Considerations in simultaneous curve fitting for repeated height-diameter measurements. *Canadian Journal of Forest Research* 24, 1408–1414. doi:10.1139/x94-181. arXiv: <http://dx.doi.org/10.1139/x94-181>.
- Fontes, L., Bontemps, J.D., Bugmann, H., Oijen, M.V., Gracia, C., Kramer, K., Lindner, M., Rötzer, T., Skovsgaard, J.P., 2010. Models for supporting forest management in a changing environment. *Forest Systems* 19, 8–29.
- Forest Products Laboratory, 1999. Wood handbook — Wood as an engineering material. General Technical Report FPL-GTR-113. U.S. Department of Agriculture, Forest Service, Forest Products Laboratory, Madison, WI. 463p.
- Forrester, D.I., 2014. The spatial and temporal dynamics of species interactions in mixed-species forests: From pattern to process. *Forest Ecology and Management* 312, 282–292. doi:10.1016/j.foreco.2013.10.003.
- Forrester, D.I., Pretzsch, H., 2015. Tamm review: On the strength of evidence when comparing ecosystem functions of mixtures with monocultures. *Forest Ecology and Management* 356, 41–53. doi:10.1016/j.foreco.2015.08.016.
- Frey, B.R., Lieffers, V.J., Hogg, E.T., Landhusser, S.M., 2004. Predicting landscape patterns of aspen dieback: mechanisms and knowledge gaps. *Canadian Journal of Forest Research* 34, 1379–1390. doi:10.1139/x04-062. arXiv: <http://www.nrcresearchpress.com/doi/pdf/10.1139/x04-062>.
- Gadow, K.v., Hui, G., 1999. Modelling Forest Development. volume 57 of *Forestry Sciences*. Kluwer Academic Publishers, Dordrecht, The Netherlands. 213 p.
- García, O., 1988. Growth modelling — a (re)view. *New Zealand Forestry* 33, 14–17.
- García, O., 1998. Estimating top height with variable plot sizes. *Canadian Journal of Forest Research* 28, 1509–1517.
- García, O., 2008. Visualization of a general family of growth functions and probability distributions — The Growth-curve Explorer. *Environmental Modelling & Software* 23, 1474–1475. doi:10.1016/j.envsoft.2008.04.005.
- García, O., 2010. Models and limits to predictability. Occasional Paper 6. University of Northern British Columbia, Natural Resources and Environmental Studies Institute, Prince George, BC, Canada.
- García, O., 2011. A parsimonious dynamic stand model for interior spruce in British Columbia. *Forest Science* 57, 265–280.
- García, O., 2013. Building a dynamic growth model for trembling aspen in western Canada without age data. *Canadian Journal of Forest Research* 43, 256–265. doi:10.1139/cjfr-2012-0366. arXiv: <http://www.nrcresearchpress.com/doi/pdf/10.1139/cjfr-2012-0366>.
- García, O., 2014a. A generic approach to spatial individual-based modelling and simulation of plant communities. *Mathematical and Computational Forestry & Natural-Resource Sciences (MCFNS)* 6, 36–47.
- García, O., 2014b. Can plasticity make spatial structure irrelevant in individual-tree models? *Forest Ecosystems* 1, 16. doi:10.1186/s40663-014-0016-1.
- García, O., Burkhart, H.E., Amateis, R.L., 2011. A biologically-consistent stand growth model for loblolly pine in the Piedmont physiographic region, USA. *Forest Ecology and Management* 262, 2035–2041. doi:10.1016/j.foreco.2011.08.047.
- Gates, D.J., O'Connor, A.J., Westcott, M., 1979. Partitioning the union of disks in plant competition models. *Proceedings of the Royal Society of London. Series A, Mathematical and Physical Sciences* 367, 59–79.

- Gradowski, T., Sidders, D., Keddy, T., Lieffers, V.J., Landhäusser, S.M., 2008. Effects of overstory retention and site preparation on growth of planted white spruce seedlings in deciduous and coniferous dominated boreal plains mixed-woods. *Forest Ecology and Management* 255, 3744–3749. doi:10.1016/j.foreco.2008.03.008.
- Grimm, V., Railsback, S.F., 2005. *Individual-Based Modeling and Ecology*. Princeton University Press, Princeton and Oxford.
- Groot, A., Gauthier, S., Bergeron, Y., 2004. Stand dynamics modelling approaches for multicohort management of Eastern Canadian boreal forests. *Silva Fennica* 38, 437–448.
- Harper, J., 1977. *Population Biology of Plants*. Academic Press.
- Hogg, E.H.T., Brandt, J.P., Michaelian, M., 2008. Impacts of a regional drought on the productivity, dieback, and biomass of western Canadian aspen forests. *Canadian Journal of Forest Research* 38, 1373–1384.
- Hu, Z., García, O., 2010. A height-growth and site-index model for interior spruce in the Sub-Boreal Spruce biogeoclimatic zone of British Columbia. *Canadian Journal of Forest Research* 40, 1175–1183. doi:10.1139/X10-075.
- Johnson, E.A., Miyanishi, K., 2008. Testing the assumptions of chronosequences in succession. *Ecology Letters* 11, 419–431. doi:10.1111/j.1461-0248.2008.01173.x.
- Jolliffe, P.A., 2000. The replacement series. *Journal of Ecology* 88, 371–385.
- Kabzems, R., Bokalo, M., Comeau, P.G., MacIsaac, D.A., 2016. Managed mixtures of aspen and white spruce 21 to 25 years after establishment. *Forests* 7, 5, 1–16. doi:10.3390/f7010005.
- Kabzems, R., García, O., 2004. Structure and dynamics of trembling aspen – white spruce mixed stands near Fort Nelson, B.C. *Canadian Journal of Forest Research* 34, 384–395.
- Kelty, M., 1992. Comparative productivity of monocultures and mixed-species stands, in: Kelty, M., Larson, B., Oliver, C. (Eds.), *The Ecology and Silviculture of Mixed-Species Forests*. Springer Netherlands. volume 40 of *Forestry Sciences*, pp. 125–141. doi:10.1007/978-94-015-8052-6_8.
- Larocque, G.R., Luckai, N., Adhikary, S.N., Groot, A., Bell, F.W., Sharma, M., 2013. Competition theory — science and application in mixed forest stands: review of experimental and modelling methods and suggestions for future research. *Environmental Reviews* 21, 71–84. doi:10.1139/er-2012-0033, arXiv:<http://www.nrcresearchpress.com/doi/pdf/10.1139/er-2012-0033>.
- Lee, M.J., García, O., 2016. Plasticity and extrapolation in modeling mixed-species stands. *Forest Science* 62, 1–8. doi:10.5849/forsci.15-027.
- Lilles, E.B., Coates, D., 2014. An evaluation of the main factors affecting yield differences between single- and mixed-species stands. *Journal of Ecosystems and Management* 14.
- Lynch, T.B., Moser, Jr., J.W., 1986. A growth model for mixed species stands. *Forest Science* 32, 697–706.
- McKinley, D.C., Ryan, M.G., Birdsey, R.A., Giardina, C.P., Harmon, M.E., Heath, L.S., Houghton, R.A., Jackson, R.B., Morrison, J.F., Murray, B.C., Pataki, D.E., Skog, K.E., 2011. A synthesis of current knowledge on forests and carbon storage in the United States. *Ecological Applications* 21, 1902–1924. doi:10.1890/10-0697.1.
- Meidinger, D., Pojar, J., 1991. *Ecosystems of British Columbia*. Special Report Series 6. BC Ministry of Forests. Victoria, BC, Canada.
- Ministry of Forests, Lands and Natural Resource Operations, 2013. TIPSYPY — Description and Use. Available on line at https://www.for.gov.bc.ca/hts/growth/tipsy/tipsy_description.html, retrieved 3 February 2016.
- Mitchell, K.J., 1975. Dynamics and simulated yield of Douglas-fir. *Forest Science Monograph* 17. Society of American Foresters.
- Mitchell-Olds, T., 1987. Analysis of local variation in plant size. *Ecology* 68, 82–87.
- Monteith, J.L., 1994. Principles of resource capture by crop stands, in: Monteith, J.L., Scott, R.K., Unsworth, M.H. (Eds.), *Resource Capture by Crops*. Proceedings of the 52nd Easter School in Agricultural Science. Nottingham University Press, Nottingham, U. K., pp. 1–15.
- Moser, Jr., J.W., Hall, O.F., 1969. Deriving growth and yield functions for uneven-aged forest stands. *Forest Science* 15, 183–188.
- Nance, W.L., Grissom, J.E., Smith, W.R., 1988. A new competition index based on weighted and constrained area potentially available, in: Ek, A.R., Shifley, S.R., Burk, T.E. (Eds.), *Forest Growth Modelling and Prediction*, USDA Forest Service, General Technical Report NC-120. pp. 134–142.
- Newnham, R.M., Smith, J.H.G., 1964. Development and testing of stand models for Douglas-fir and lodgepole pine. *The Forestry Chronicle* 40, 494–504.
- Nigh, G., 2002. Site index conversion equations for mixed trembling aspen and white spruce stands in northern British Columbia. *Silva Fennica* 36, 789–797.
- Perry, D.A., 1985. The competition process in forest stands, in: Cannell, M.G.R., Jackson, J.E. (Eds.), *Attributes of Trees as Crop Plants*. Institute of Terrestrial Ecology, Abbots Ripton, Hunts, England. chapter 28, pp. 481–506.
- Pretzsch, H., 2009. *Forest Dynamics, Growth and Yield: From Measurement to Model*. Springer, Berlin.
- Pretzsch, H., Forrester, D.I., Rtzer, T., 2015. Representation of species mixing in forest growth models. A review and perspective. *Ecological Modelling* 313, 276 – 292. doi:10.1016/j.ecolmodel.2015.06.044.
- R Development Core Team, 2009. *R: A Language and Environment for Statistical Computing*. R Foundation for

- Statistical Computing. Vienna, Austria. ISBN 3-900051-07-0 (<http://www.R-project.org>).
- Reventlow, C.D.F., 1879. A Treatise of Forestry. Society of Forest History, Horsholm, Denmark. (English translation, 1960).
- del Río, M., Pretzsch, H., Alberdi, I., Bielak, K., Bravo, F., Brunner, A., Condés, S., Ducey, M.J., Fonseca, T., von Lpke, N., Pach, M., Peric, S., Perot, T., Souidi, Z., Spathelf, P., Sterba, H., Tijardovic, M., Tomé, M., Vallet, P., Bravo-Oviedo, A., 2016. Characterization of the structure, dynamics, and productivity of mixed-species stands: review and perspectives. *European Journal of Forest Research* 135, 23–49. doi:10.1007/s10342-015-0927-6.
- Russell, M.B., D'Amato, A.W., Albers, M.A., Woodall, C.W., Puettmann, K.J., Saunders, M.R., VanderSchaaf, C.L., 2015. Performance of the Forest Vegetation Simulator in managed white spruce plantations influenced by Eastern spruce budworm in Northern Minnesota. *Forest Science* 61, 723–730. doi:10.5849/forsci.14-150.
- Salas, C., Stage, A.R., Robinson, A.P., 2008. Modeling effects of overstory density and competing vegetation on tree height growth. *Forest Science* 54, 107–122.
- Salas, J.D., Kim, H.S., Eykholt, R., Burlando, P., Green, T.R., 2005. Aggregation and sampling in deterministic chaos: implications for chaos identification in hydrological processes 12, 557–567.
- Sambakhe, D., Fortin, M., Renaud, J.P., Deleuze, C., Dreyfus, P., Picard, N., 2014. Prediction bias induced by plot size in forest growth models. *Forest Science* 60, 1050–1059. doi:10.5849/forsci.13-070.
- Sayama, H., 2015. Modeling and Analysis of Complex Systems. Open SUNY Textbooks, Milne Library, State University of New York, Geneseo, NY.
- Seber, G.A.F., Wild, C.J., 2003. *Nonlinear Regression*. Wiley-Interscience, New York. 768 p.
- Simon, H.A., 1962. The architecture of complexity. *Proceedings of the American Philosophical Society* 106, 467–482.
- Soetaert, K., Petzoldt, T., Setzer, R.W., 2010. Solving differential equations in R package deSolve. *Journal of Statistical Software* 33, 1–25.
- Staebler, G.R., 1951. Growth and Spacing in an Even-aged Stand of Douglas-Fir. Master's thesis. School of Natural Resources, University of Michigan.
- Sterba, H., del Río, M., Brunner, A., Condés, S., 2014. Effect of species proportion definition on the evaluation of growth in pure vs. mixed stands. *Forest Systems* 23.
- Strigul, N., Pristinski, D., Purves, D., Dushoff, J., Pacala, S., 2008. Scaling from trees to forests: Tractable macroscopic equations for forest dynamics. *Ecological Monographs* 78, 523–545.
- Vanclay, J., Skovsgaard, J., 1997. Evaluating forest growth models. *Ecological Modelling* 98, 1–12.
- Venables, W.N., Ripley, B.D., 2002. *Modern Applied Statistics with S*. Fourth ed., Springer, New York. 495 p.
- Weiskittel, A.R., Crookston, N.L., Radtke, P.J., 2011a. Linking climate, gross primary productivity, and site index across forests of the western United States. *Canadian Journal of Forest Research* 41, 1710–1721. doi:10.1139/x11-086, arXiv:<http://www.nrcresearchpress.com/doi/pdf/10.1139/x11-086>.
- Weiskittel, A.R., Hann, D.W., John A. Kershaw, J., Vanclay, J.K., 2011b. *Forest Growth and Yield Modeling*. Wiley-Blackwell. 430 p.
- de Wit, C.T., 1960. On Competition. *Versl.Landbouwk. Onderzoek*. 66.8. Institute for Biological and Chemical Research on Field Crops and Herbage. Wageningen, The Netherlands. 82 p.
- de Wit, C.T., van den Bergh, J.P., 1965. Competition between herbage plants. *Neth. J. Agric. Sci.* 13, 212–221.
- Worrall, J.J., Rehfeldt, G.E., Hamann, A., Hogg, E.H., Marchetti, S.B., Michaelian, M., Gray, L.K., 2013. Recent declines of *Populus tremuloides* in North America linked to climate. *Forest Ecology and Management* 299, 35–51. doi:10.1016/j.foreco.2012.12.033.
- Zingg, A., 1994. Top heights in mixed stands: their definition and calculation, in: Pinto da Costa, M.E., Preuhler, T. (Eds.), *Mixed Stands. Reserach Plots, Measurements and Results, Models*, Universidade Técnica de Lisboa, Instituto Superior de Agronomia, Lisboa, Portugal. pp. 67–79.